

NO_x Emission Reduction and its Effects on Ozone during the 2008 Olympic Games

Qing Yang,^{*,†,‡,||} Yuhang Wang,[†] Chun Zhao,[‡] Zhen Liu,[†] William I. Gustafson, Jr.,[‡] and Min Shao[§]

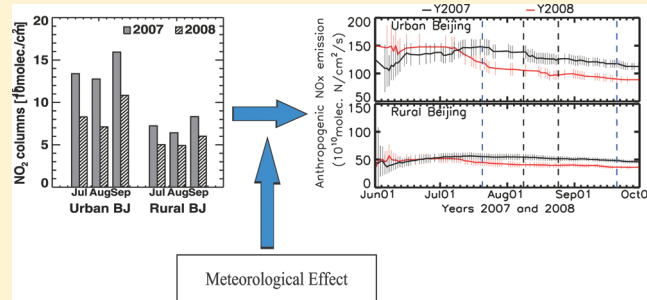
[†]School of Earth and Atmospheric Sciences, Georgia Institute of Technology, 311 Ferst Drive, Atlanta, Georgia, United States

[‡]Atmospheric Sciences and Global Change Division, Pacific Northwest National Laboratory, Richland, Washington, United States

[§]College of Environmental Sciences and Engineering, Peking University, Beijing, China

S Supporting Information

ABSTRACT: We applied a daily assimilated inversion method to estimate NO_x (NO + NO₂) emissions for June–September 2007 and 2008 on the basis of the Aura Ozone Monitoring Instrument (OMI) observations of nitrogen dioxide (NO₂) and model simulations using the Regional Chemistry and Transport Model (REAM). This method allows for estimating emission changes with a finer temporal resolution than previous studies and shows that the progression of the emission reduction corresponds roughly to the scheduled implementation of emission controls over Beijing. OMI column NO₂ reductions are approximately 45%, 33%, and 14% over urban Beijing, rural Beijing, and the Huabei Plain, respectively, while the corresponding anthropogenic NO_x emission reductions are only 28%, 24%, and 6%, during the full emission control period (July 20–Sep 20, 2008). Meteorological changes from summer 2007 to 2008 are the main factor contributing to the column NO₂ decreases not accounted for by the emission reduction. The surface ozone changes due to NO_x emission reduction are negligible using a standard VOC emission inventory. When using enhanced VOC (particularly aromatics) emissions derived from in situ observations, urban Beijing shifted O₃ production from the VOC-limited regime toward the NO_x-limited regime resulting in a more substantial ozone decrease (up to 10 ppbv).



1. INTRODUCTION

The 2008 Olympics and Paralympics were held in Beijing during August 8–24 and September 9–17, 2008, respectively. Large efforts were undertaken by the city of Beijing and the surrounding provinces to mitigate the air pollution of Beijing during the Olympic Games through emission abatement, by targeting traffic, power plants, and some industries on local and regional scales. The period with full emission control extended from July 20 to September 20 in 2008, with partial emission controls as early as July 1. Motor vehicles during the full control period were permitted to drive only on alternative days and a large number of factories and power plants with high emissions were required to stop emissions or cut their emissions by 30%.¹ Moderate restrictions were also implemented in some neighboring cities.

In several recent papers, air quality related to NO₂ concentrations and the nitrogen oxides (NO_x = NO + NO₂) emissions during the 2008 Olympics were studied. Based on the Aura Ozone Monitoring Instrument (OMI) satellite observations alone, Witte et al.² estimated a 43% reduction in tropospheric column NO₂ during the 2008 Olympics compared to the averages of the past three years. In situ observations of gas concentrations at a rural site 100 km downwind of the Beijing urban center were used by Wang et al.¹ to study the air quality

during the 2008 Beijing Olympics. They estimated a NO_x emission reduction of 36% from 2007 to 2008 during August. The reduction of NO₂ concentrations, however, reflects not only the emission reduction in Beijing but also the decrease of NO₂ from June to August when photochemistry becomes more active and the lifetime of NO_x becomes shorter. Wang et al.³ and Zhou et al.⁴ used a bottom-up methodology and arrived at a mobile source NO_x emission reduction of 46% during the Beijing Olympics. However, the uncertainties associated with the more traditional bottom-up approach are, in general, large, and top-down inversion approaches are able to reduce those uncertainties.⁵

The reduction in tropospheric NO₂ concentrations is not equivalent to NO₂ emission reduction due to the presence of chemical feedbacks involving hydroxyl radicals (OH).⁶ When the emission change is as large as 30–40%, the chemical feedback effect could be important.⁷ Analysis from this study also suggests non-negligible impacts of year-to-year variation in meteorological conditions to the NO₂ column amount changes in two

Received: February 26, 2011

Accepted: June 20, 2011

Revised: June 7, 2011

Published: June 20, 2011

years. In this study, we applied a more robust top-down approach, the daily assimilated inversion scheme, which was improved from the monthly inversion by Martin et al.⁵ by taking advantage of the available high-resolution tropospheric NO₂ columns from OMI.⁸ The iterative nature of the assimilated inversion has an advantage over the widely used monthly mean inversion by accounting for chemical feedbacks of the changed NO_x emission, and it reduces the dependence of the *a posteriori* inventory on the *a priori* emissions.⁸

In this study, the daily assimilated inversion method allows for examining the timing of the emission reduction at a much better temporal resolution than previous studies (e.g., refs 1,9). The objectives of this study are 2-fold: (1) to quantify the changes in observed NO₂ columns and the corresponding reduction in the anthropogenic surface NO_x emissions over Beijing and other regions in China during the 2008 Olympics/Paralympics emission control period; and (2) to assess the impacts of the NO_x/VOC (volatile organic compounds) emission reductions on surface ozone concentrations through model sensitivity analysis.

2. DATA AND METHODS

2.1. Satellite Data. OMI is a nadir viewing, near-UV and visible spectrograph, which is onboard the Aura satellite. Although two subsequent Aura orbits are ~16° apart in longitude, OMI relies on the wide cross track ground swath (~2600 km, 60 pixel scans) to provide daily global maps of NO₂ measurements with a medium pixel size of 760 km² over Beijing.¹⁰ One tropospheric NO₂ column datum is retrieved for each OMI pixel over the sun-lit portion (~15:00 local time over eastern China) of the orbits. Two independent OMI tropospheric NO₂ column products are available: a product retrieved by the NASA Goddard Space Flight Center and a product retrieved by the Royal Dutch Meteorological Institute, referred to as Goddard and KNMI products, respectively, hereafter. The validation of the Goddard and KNMI products can be found in a few papers (e.g., refs 11–14 for the Goddard products and 15 for the KNMI products). Significant differences were reported between the two products: Bucsla et al.¹¹ reported KNMI and Goddard NO₂ columns are 14 ± 20% lower and 68 ± 60% higher, respectively, than in situ aircraft measurements of NO₂ columns. In addition, Lamsal et al.¹⁶ found a particularly high summer bias of the Goddard columns over North America, although the difference between the two products is smaller over China.⁸ Following Zhao and Wang,⁸ the error-weighted averages of the two products were used for this study. Clear sky level 2 tropospheric NO₂ columns for both KNMI (version 1.0.3) and Goddard products (version 3) were gridded to the Regional chemistry and transport Model (REAM) grids (70 km × 70 km). Only level II data with a cloud fraction of less than 20% were included. Sensitivity tests using different cloud fraction thresholds are discussed in the Supporting Information. Data associated with the OMI cross-track row anomaly were excluded in this study. Because more data were removed in 2008 due to the additional rows of anomaly in 2008, the amount of available satellite NO₂ column data in 2008 is about 15% less than that of 2007. Consequently, as shown later, the inverted emission time series over urban Beijing in 2008 is more acutely affected by missing satellite data.

Based on the gridded clear sky data, the differences between the two satellite NO₂ retrieval products (Goddard and KNMI) are consistently around 0.5 ± 2.2 × 10¹⁵ molec./cm² over

Beijing and over the Huabei Plain for June–September 2007 and 2008. The correlation coefficients between the two products are approximately 0.9. A description of the uncertainty estimation of the error-weighted averages used in this study is provided in the Supporting Information. Detailed investigations of the differences in the two products are beyond the scope of this study; however, the sensitivity of the *a posteriori* emissions to the use of the two different NO₂ products has been investigated and the results are presented in the Supporting Information.

2.2. REAM Model. REAM is a 3-D regional chemical transport model. A number of studies (e.g., refs 17–21) on effects of lightning and convection, trans-Pacific transport, polar tropospheric chemistry, and Asian monsoon have been based on REAM simulations. The model's chemistry and deposition modules are adopted from the GEOS-Chem model with the addition of the SAPRC-07 aromatics-oxidation mechanism.²² The 1-D version of REAM was applied to analyze in situ observations in Beijing in August 2007 and good agreement was found when aromatics chemistry was included.²³ The initial and boundary conditions of the tracer concentrations are obtained from GEOS-Chem (version 8.1) with boundary conditions updated hourly. In this study, the model is driven by meteorological data from the Weather Research and Forecasting Model (WRF version 3.1). REAM has a horizontal resolution of 70 km × 70 km, and 23 vertical layers between the surface and the model upper boundary (10 hPa). Because the average OMI pixel width is ~50 km over Beijing, the model horizontal resolution is adequate for the inversion modeling of NO_x emissions using OMI NO₂ column measurements and for studying the effects of OMI derived NO_x emission changes over the Beijing region.

The lightning NO_x emission is parameterized as by Choi et al.²⁰ The algorithm of soil NO_x emissions follows Wang et al.²⁴ in which an algorithm by Yienger and Levy²⁵ was adopted. The anthropogenic emissions of tracers other than NO_x are based on the 2006 Asian emission inventory (referred to as Streets 2006 inventory hereafter)²⁶ developed in support of NASA's INTEX-B (Intercontinental Chemical Transport Experiment) mission.

2.3. Inverse Modeling. The top-down inversion framework follows that by Zhao and Wang⁸ with an improvement in the uncertainty analysis for the purpose of obtaining a *a posteriori* emissions on a daily scale. A top-down NO_x emission is obtained by scaling the *a priori* emission by the ratio of the observed to simulated tropospheric NO₂ columns. After error analysis, an optimized emission is calculated by error-weighted averaging of the top-down emission inventory and the *a priori* emission inventory. The obtained *a posteriori* emission and errors are then used as the *a priori* estimates for the next day. This process iterates daily at the satellite pass time. A detailed method description and convergence analysis can be found elsewhere.⁸ Daily assimilated inversion of source NO_x was conducted continuously from June 1 to September 30 for both 2007 and 2008. More discussion related to the uncertainty analysis and the inversion method is provided in the Supporting Information.

3. RESULTS AND DISCUSSION

3.1. Observed Column Reductions. To facilitate the discussion of NO_x emission changes, we first define 5 regions: urban Beijing, rural Beijing, the Huabei Plain, Northeastern China, and Southeastern China (Figure 1). The observed changes in tropospheric NO₂ columns were calculated by comparing OMI

retrievals during the Olympic emission control period (July 20–September 20, 2008) with those during the same time period in 2007 (Table 1). Similar comparisons based on monthly averages are shown in Figure S1 of the Supporting Information. Consistent with the previous study,² the average reduction is approximately 45% over urban Beijing, 33% over rural Beijing, 14% over the Huabei Plain, 8% over northeast China, and 9% over southeast China during the full emission control period. The reductions in 2008, compared to 2007, are substantially greater over urban and rural Beijing than the other regions.

3.2. Estimated Reductions in NO_x Emissions. The daily assimilated inversion method enables us to investigate the temporal progression of NO_x emission reductions during the Olympics period (Figure 2), which has not yet been examined using atmospheric observations. Larger uncertainties in the time series over urban Beijing is partly because the other regions include a larger number of grid boxes for the averages. The convergence time of the assimilated inversion is 3–5 days⁸ and therefore the estimated emission change could have a time lag of several days although the onset of the emission change should be captured by the inversion. An issue in the inversion is related to missing satellite data due to either cloud interference or the row anomaly (more rows affected in 2008) of the OMI instrument. The missing data issue is more acute for small regions such as urban Beijing. We compared the results with and without the removal of the row anomaly and found that the results are consistent. The results presented here are based on the data with the row anomaly pixels removed.

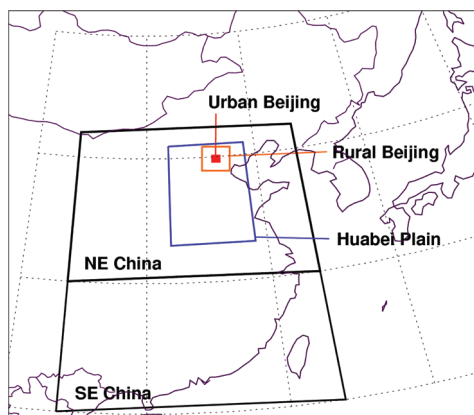


Figure 1. Urban Beijing is defined as the 70 km × 70 km region centered at 39.97° N and 116.35° E (the red filled box). Rural Beijing and the Huabei Plain (33°–41° N and 112°–119° E) are indicated by the orange and blue boxes, respectively. The upper and lower black boxes are defined as northeastern China (30°–42° N and 113.75°–123.75° E) and southeastern China (20°–30° N and 113.75°–123.75° E), respectively. Each region is mutually exclusive and only includes continental areas.

The partial emission control was scheduled to start as early as July 1 and the full control was scheduled on July 20 in 2008. In comparison, the inversion results in Figure 2 show a late onset of July 12 over urban Beijing. Missing data on June 22–July 2 and July 4–July 11 affected the inversion results, but the results indicate that the effect of initial partial emission control measures (e.g., banning 70% of government-owned vehicles and power plants reducing their emission by 30% from their June level³) is relatively small on NO_x emission. The inversion results show a rapid reduction of NO_x emissions starting on July 12 and the reduction reached its maximum on July 23, implying that the full emission control measures went into effect a week or so before the scheduled deadline of July 20. Rural Beijing is affected less by the missing data due to averaging over a larger region. The inversion results over rural Beijing corroborate those over urban Beijing. The emission reduction between June 22 and July 1 was negligible. A minor decrease in emission was evident after July 1, but the effect is relatively small until July 12. The full emission control effect was more significant about 1 week before July 20 as in urban Beijing. Another noticeable decrease of NO_x emissions over urban Beijing is found around August 15, which may reflect

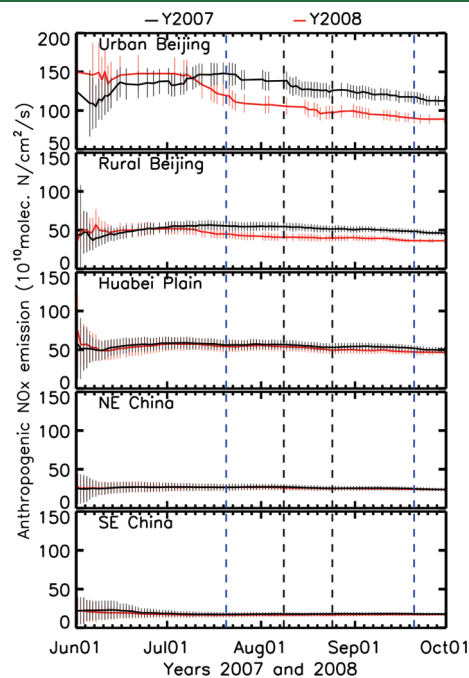


Figure 2. Time series of estimated anthropogenic NO_x emissions over 5 defined regions. Uncertainties ($\pm 2\sigma$) are shown by the vertical bars. The black dashed vertical lines bound the duration of the Olympic Games (August 8–24, 2008), and the blue dashed vertical lines bound the full emission control period (July 20–September 20, 2008).

Table 1. Changes in Observed NO₂ and Anthropogenic NO_x Emissions between 2007 and 2008 for the Emission Control Period (July 20–September 20)

	Urban Beijing	Rural Beijing	Huabei Plain	NE China	SE China
observed column NO ₂ change	−44.7% (−7.4 ^a)	−32.6% (−2.4 ^a)	−14.1% (−1.0 ^a)	−7.6% (−0.3 ^a)	−8.9% (−0.2 ^a)
estimated emission change ^c	−28.2 ± 8.2% (−38.4 ± 9.4 ^b)	−23.9 ± 9.8% (−9.9 ± 4.4 ^b)	−6.0 ± 10.2% (−3.5 ± 5.4 ^b)	−1.6 ± 11.8% (−0.4 ± 3.0 ^b)	−6.7 ± 12.8% (−1.2 ± 2.2 ^b)

^a Absolute column change in unit of 1×10^{15} molec. cm^{−2}. ^b Absolute emission change in unit of 1×10^{15} molec. N cm^{−2} s^{−1}. ^c The uncertainty of the emission change is estimated as $\pm 2\sigma$, where σ is the estimated error of the emission.

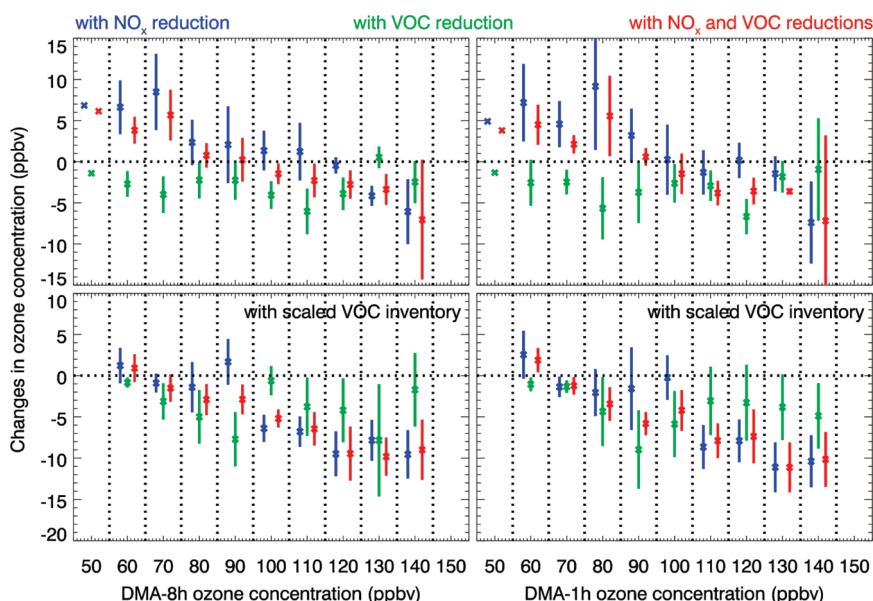


Figure 3. Changes of DMA-8h (left) and DMA-1h (right) ozone due to emission reductions. The standard (top row) and scaled (bottom row) VOC inventories were used, respectively, for three emission reduction scenarios: NO_x only (blue), VOC only (green), and both NO_x and VOC emission reductions (red). The vertical bars indicate the uncertainties ($\pm 2\sigma$).

the additional 10% cut in power plant emissions scheduled at the opening of the Olympics Games on August 8. Satellite data were missing on August 4–14 over urban Beijing, so the exact timing might not be correctly reflected. The additional reduction measure after August 8 does not appear to affect rural Beijing and other regions.

During the emission control period, the anthropogenic NO_x emissions are reduced by approximately $28 \pm 8\%$ and $24 \pm 10\%$ over urban and rural Beijing, respectively, and by $6 \pm 10\%$ over the Huabei Plain, $2 \pm 12\%$ over NE China, and $7 \pm 13\%$ over SE China as compared to the same period in 2007 (Table 1). The uncertainty of the emission change is estimated as $\pm 2\sigma$, where σ is the estimated error of the emission. The emission reductions over urban and rural Beijing are statistically significant (defined by the 95% confidence interval) after July 20. Except for a few days in September over the Huabei Plain, the emission reductions are not statistically significant over the Huabei Plain, NE China, and SE China.

The average emission rates over rural Beijing are similar to those of the Huabei Plain in 2007 and are lower than those of the Huabei Plain after the emission reduction in 2008. The emissions over urban Beijing have the largest reduction in 2008 but are still much higher than those of rural Beijing and the Huabei Plain. After the Paralympics, the emissions did not appear to increase back to the 2007 level. Detailed spatial distributions of the emission reduction over Beijing and surrounding regions are included in the Supporting Information (Figure S3).

Over urban Beijing, the estimated emission reduction is 28%, which is significantly less than the satellite-observed column reduction of 45%. To understand the difference between the emission and column change, we quantified the effects of soil NO_x emissions, lightning NO_x production, and meteorology (Table S2 in the Supporting Information). The overall effects of meteorology were estimated by comparing the two simulations using the same emission but driven by 2007 and 2008 meteorology, respectively. Soil NO_x emission amounts are

similar in the two years, but due to the larger *a posteriori* NO_x emission in 2007, when expressed in percentage, soil NO_x is higher by 2% in 2008 over urban Beijing. Four percent of the column difference was due to lightning-produced NO_x, the uncertainty of which is very large. Among the three factors, the combined effect of soil emissions and lightning production is small. The main effect is due to meteorological changes from 2007 to 2008. Meteorological conditions account for 12% of the column difference in the same period between the two years over urban Beijing. For example, the boundary layer ventilation coefficient, which is defined as boundary layer height times mean boundary layer wind speed,²⁷ is approximately 5% higher in 2008 versus 2007 during the emission control period. Additionally, there were more sunny days in 2008 (25%) compared to 2007 (21%), resulting in more photochemical oxidation. Both factors contribute to the reduction in tropospheric NO₂ columns. In general, the emission change is less than the NO₂ column change because of the chemical feedback of NO_x on OH.⁶ The results of similar analyses for other regions are also shown in the Supporting Information (Table S2).

3.3. Effectiveness of Emission Reductions on Ozone. The 28% reduction in NO_x emissions demonstrates the effectiveness of emission reduction mandates by the Chinese government considering what can be reasonably achieved through abatement measures in such a short period of time. We apply model sensitivity simulations to examine the effectiveness of emission reductions on surface ozone concentrations from July to September 2008. Three sensitivity simulations were conducted as follows: (1) with the anthropogenic NO_x emission reduction only, (2) with the anthropogenic VOC emission reduction only, and (3) with both anthropogenic NO_x and VOC emission reductions. In the base simulations, the 2007 anthropogenic NO_x emissions (obtained through assimilated inversion) and the Streets 2006 VOC inventory were used. In the reduction simulations, the 2007 anthropogenic NO_x emissions were replaced by the 2008 NO_x emissions (obtained through assimilated inversion).

Table 2. Changes in DMA-8h and DMA-1h Ozone Concentrations Due to Emission Reductions for Three Emission Reduction Scenarios: NO_x Only, VOC Only, and Both NO_x and VOC Emission Reductions

	VOC emissions	NO _x emission reduction (ppbv)		VOC emission reduction (ppbv)		NO _x /VOC emission reduction (ppbv)	
		mean/std all	mean/std high ^b	mean/std all	mean/std high ^b	mean/std all	mean/std high ^b
DMA-8h	w/o scaling ^a	3.0/0.8	-0.2/0.7	-3.3/0.4	-3.4/0.5	0.7/0.6	-2.3/0.5
	w. scaling ^a	-4.4/0.7	-5.6/0.8	-4.5/0.7	-5.2/0.9	-5.5/0.6	-6.8/0.6
DMA-1h	w/o scaling ^a	2.1/0.9	-2.0/0.7	-3.4/0.4	-3.6/0.6	-0.4/0.6	-4.4/0.5
	w. scaling ^a	-5.7/0.7	-9.5/0.7	-4.5/0.7	-4.6/1.1	-6.7/0.6	-9.8/0.8

^a "w/o scaling" denotes simulations using the Streets 2006 VOC inventory. "w. scaling" denotes the VOC inventory scaled to reproduce VOC measurements during the CAREBEIJING-2007 experiment. ^b For high ozone data with DMA-8h > 75 ppbv or DMA-1h > 110 ppbv in the base simulation.

The amount of VOC emission reduction was estimated by scaling the estimated NO_x reduction with a VOC-to-NO_x reduction ratio during the 2008 Olympics estimated by Wang et al.³

We compared the simulations with emission reductions to base simulations to investigate how daily maximum average 8-h or 1-h surface ozone (O₃) (DMA-8h or DMA-1h) are affected (Figure 3 and Table 2).

The difference between VOC and NO_x reductions is quite large. VOC reductions lead to a several ppbv decrease of O₃ independent of the ambient O₃ concentrations. NO_x reduction, in contrast, decreases O₃ when DMA-8h or DMA-1h O₃ concentrations are above 75 ppbv and 100 ppbv, respectively, but increases O₃ when ambient O₃ concentrations are lower. The mean DMA-8h and DMA-1h O₃ concentrations increased 3.0 ± 0.8 and 2.1 ± 0.9 ppbv, respectively, due to the NO_x emission reduction during the full emission control period in 2008 in urban Beijing (Table 2). In contrast, they decreased 3.3 ± 0.4 and 3.4 ± 0.4 ppbv, respectively, due to the VOC emission reduction. This behavior is usually referred to as the VOC-limited regime (e.g., ref 28 for metro Mexico City).

The general trend of concurrent NO_x and VOC reductions is similar to that of the NO_x reduction alone. When NO_x and VOC emissions are concurrently reduced, the changes in the mean DMA-8h and DMA-1h are small. They are both not statistically different from 0 (0.7 ± 0.6 and -0.4 ± 0.6 ppbv, respectively). Although concurrent reduction led to modest decreases during high ozone episodes: approximately 2.3 ± 0.5 ppbv and 4.4 ± 0.5 ppbv drops in DMA-8h and DMA-1h, respectively. Exceedances over the U.S. ozone DMA-8 h standard of 75 ppbv, and over Chinese level 1–3 ambient air hourly O₃ standards (60, 100, and 120 μg/m³ or roughly 80, 100, 120 ppbv) were affected very little by the emission reductions (Figure 3). The changes in surface ozone production rates due to emission reductions during the daytime (see Figure S5 in the Supporting Information) are consistent with the changes in DMA-8h and DMA-1h ozone concentrations. Reducing NO_x emission accelerates ozone production by 0.4 ppbv/h, while VOC emission reduction decreases the rate by 0.8 ppbv/h. The reduction in both emissions reduces ozone production by only 0.3 ppbv/h.

Before a conclusion is drawn on the relatively small overall impacts of NO_x and VOC emission reductions on surface ozone, we note that there are large uncertainties in the VOC emission inventory for China.²⁰ By comparing the VOC concentrations from the base model simulation with those measured in the CAREBEIJING-2007 Experiment during August 2007,²⁰ we found severe underestimations of the anthropogenic VOC emissions over Beijing. Model sensitivity simulations suggest

scaling factors of 5 and 7, respectively, are needed for model tracers ARO1 (benzene, ethyl-benzene, and toluene) and ARO2 (all other aromatics other than those in ARO1) in the current Streets 2006 VOC inventory. Due to the nonlinearity of ozone photochemistry, the large increase of VOC emissions in urban Beijing shifted O₃ production away from the VOC-limited regime toward the NO_x-limited regime, and the emission reduction effects are more significant. NO_x-limited ozone production regime has been reported for urban areas such as Tokyo²⁹ and Chicago.³⁰

The simulated mean DMA-8h and DMA-1h ozone concentrations decreased, by 5.5 ± 0.6 and 6.7 ± 0.6 ppbv, respectively, and decreased by 6.8 ± 0.6 and 9.8 ± 0.8 ppbv during high ozone episodes (>75 ppbv in DMA-8h or >100 ppbv in DMA-1h) in urban Beijing (Figure 3). Table 2 summarizes the drastic changes for the scenarios of NO_x only and NO_x+VOC reductions, both of which show much larger reductions in surface ozone. Hence, an accurate assessment of the impacts of 2008 Olympic emission control measures on surface ozone is hindered by the uncertainties in the VOC emission inventory.

Additional sensitivity runs on impacts of the regional emission by turning off NO_x and VOC emissions over the Huabei Plain including metro Beijing (see Supporting Information for details) agree with conclusions by Streets et al.³¹ that the emissions over the Huabei Plain exert significant impacts on the ozone air quality over urban Beijing. Due to the nonlinearity of ozone chemical processes, limiting emissions over only the metro Beijing area may not lead to overall reductions in surface ozone concentrations. It appears to be necessary to conduct emission controls over a more extensive area to make the emission control more effective. Therefore, the relatively small impact on surface ozone of regulating NO_x/VOC emissions might also be related to the limited area (metro Beijing and surrounding cities) of the emission control during the 2008 Olympics.

■ ASSOCIATED CONTENT

Supporting Information. (1) Detailed descriptions of the assimilated method. (2) Sensitivity of the NO₂ columns to the cloud fraction thresholds. (3) Observed NO₂ column reduction. (4) Sensitivity of assimilated emissions to the use of Goddard and KNMI products. (5) Sensitivity of the assimilated emissions to soil NO_x emission, lightning NO_x production and meteorology. (6) Spatial distribution of the NO_x emission reduction. (7) Impacts of the regional emission. (8) Two tables and five additional figures (Figure S1–S5). This material is available free of charge via the Internet at <http://pubs.acs.org>.

AUTHOR INFORMATION

Corresponding Author

*Phone: (509)-372-4650; fax: (509)-372-6168; e-mail: qing.yang@pnnl.gov.

Present Addresses

^{||}Atmospheric Sciences and Global Change Division, Pacific Northwest National Laboratory, Richland, WA.

ACKNOWLEDGMENT

This work was supported by the National Science Foundation Atmospheric Chemistry Program.

REFERENCES

- (1) Wang, Y.; Hao, J.; McElroy, M. B.; Munger, J. W.; Ma, H.; Chen, D.; Nielsen, C. P. Ozone air quality during the 2008 Beijing Olympics: Effectiveness of emission restrictions. *Atmos. Chem. Phys.* **2009**, *9*, 5237–5251.
- (2) Witte, J. C.; Schoeberl, M. R.; Douglass, A. R.; Gleason, J. F.; Krotkov, N. A.; Gille, J. C.; Pickering, K. E.; Livesey, N. Satellite observations of changes in air quality during the 2008 Beijing Olympics and Paralympics. *Geophys. Res. Lett.* **2009**, *36*, L1780310.1029/2009GL039236.
- (3) Wang, S.; Zhao, M.; Xing, J.; Wu, Y.; Zhou, Y.; Lei, Y.; He, K.; Fu, L.; Hao, J. Quantifying the air pollutants emission reduction during the 2008 Olympic Games in Beijing. *Environ. Sci. Technol.* **2010**, *44*, 2490–2496 10.1021/es9028167.
- (4) Zhou, Y.; Wu, Y.; Yang, L.; Fu, L.; He, K.; Wang, S.; Hao, J.; Chen, J.; Li, C. The impact of transportation control measures on emission reductions during the 2008 Olympic Games in Beijing, China. *Atmos. Environ.* **2010**, *44*, 285–293 10.1016/j.atmosenv.2009.10.040.
- (5) Martin, R. V.; Jacob, D. J.; Chance, K.; Kurosu, T. P.; Palmer, P. I.; Evans, M. J. Global inventory of nitrogen oxide emissions constrained by space-based observations of NO₂ columns. *J. Geophys. Res.* **2003**, *108* (D17), 453710.1029/2003JD003453.
- (6) van der A, R. J.; Eskes, H. J.; Boersma, K. F.; van Noije, T. P. C.; Van Roozendael, M.; De Smedt, I.; Peters, D. H. M. U.; Meijer, E. W. Trends, seasonal variability and dominant NO_x source derived from a ten year record of NO₂ measured from space. *J. Geophys. Res.* **2008**, *113*, D0430210.1029/2007JD009021.
- (7) Lamsal, L. N.; Martin, R. V.; Padmanabhan, A.; van Donkelaar, A.; Zhang, Q.; Sioris, C. E.; Chance, K.; Kurosu, T. P.; Newchurch, M. J. Application of satellite observations for timely updates to global anthropogenic NO_x emission inventories. *Geophys. Res. Lett.* **2011**, *38*, L0581010.1029/2010GL046476.
- (8) Zhao, C.; Wang, Y. Assimilated inversion of NO_x emissions over Asia using OMI NO₂ column measurements. *Geophys. Res. Lett.* **2009**, *36*, L0680510.1029/2008GL037123.
- (9) Mijling, B.; van der A, R. J.; Boersma, K. F.; Van Roozendael, M.; De Smedt, I.; Kelder, H. M. Reductions of NO₂ detected from space during the 2008 Beijing Olympic Games. *Geophys. Res. Lett.* **2009**, *36*, L1380110.1029/2009GL038943.
- (10) Yang, Q.; Cunnold, D. M.; Wang, H.-J.; Froidevaux, L.; Claude, H.; Merrill, J.; Newchurch, M.; Oltmans, S. J. Midlatitude tropospheric ozone columns derived from the Aura Ozone Monitoring Instrument and Microwave Limb Sounder measurements. *J. Geophys. Res.* **2007**, *112*, D2030510.1029/2007JD008528.
- (11) Bucsela, E. J.; Perring, A. E.; Cohen, R. C.; Boersma, K. F.; Celarier, E. A.; Gleason, J. F.; Wening, M. O.; Bertram, T. H.; Wooldridge, P. J.; Dirksen, R.; Veefkind, J. P. Comparison of tropospheric NO₂ from in situ aircraft measurements with near-real-time and standard product data from OMI. *J. Geophys. Res.* **2008**, *113*, D16S3110.1029/2007JD008838.
- (12) Brinkma, E. J.; Pinardi, G.; Volten, H.; Braak, R.; Richter, A.; Schönhardt, A.; van Roozendael, M.; Fayt, C.; Hermans, C.; Dirksen,

R. J.; Vlemmix, T.; Berkhout, A. J. C.; Swart, D. P. J.; Oetjen, H.; Wittrock, F.; Wagner, T.; Ibrahim, O. W.; de Leeuw, G.; Moerman, M.; Curier, R. L.; Celarier, E. A.; Cede, A.; Knap, W. H.; Veefkind, J. P.; Eskes, H. J.; Allaart, M.; Rothe, R.; PETERS, A. J. M.; Levelt, P. F. The 2005 and 2006 DANDELIONS NO and aerosol intercomparison campaigns. *J. Geophys. Res.* **2008**, *113*, D16S4610.1029/2007JD008808.

(13) Wening, M. O.; Cede, A. M.; Bucsela, E. J.; Celarier, E. A.; Boersma, K. F.; Veefkind, J. P.; Brinkma, E. J.; Gleason, J. F.; Herman, J. R. Validation of OMI tropospheric NO₂ column densities using direct sun mode Brewer measurements at NASA Goddard Space Flight Center. *J. Geophys. Res.* **2008**, *113*, D16S4510.1029/2007JD008988.

(14) Bucsela, E. J.; Celarier, E. A.; Wening, M. O.; Gleason, J. F.; Veefkind, J. P.; Boersma, K. F.; Brinkma, E. J. Algorithm for NO₂ vertical column retrieval from the Ozone Monitoring Instrument. *IEEE Trans. Geosci. Remote Sens.* **2006**, *44*, 1245–1258.

(15) Boersma, K. F.; Jacob, D. J.; Bucsela, E. J.; Perring, A. E.; Dirksen, R.; van der A, R. J.; Yantosca, R. M.; Park, R. J.; Wening, M. O.; Bertram, T. H.; Cohen, R. C. Validation of OMI tropospheric NO₂ observation during INTEX-B and application to constrain NO_x emissions over the eastern United States and Mexico. *Atmos. Environ.* **2008**, *42*, 4480–4497.

(16) Lamsal, L. N.; Martin, R. V.; van Donkelaar, A.; Celarier, E. A.; Bucsela, E. J.; Boersma, K. F.; Dirksen, R.; Luo, C.; Wang, Y. Indirect validation of tropospheric nitrogen dioxide retrieved from the OMI satellite instrument: Insight into the seasonal variation of nitrogen oxides at northern midlatitudes. *J. Geophys. Res.* **2010**, *115*, D0530210.1029/2009JD013351.

(17) Zhao, C.; Wang, Y.; Choi, Y.; Zeng, T. Summertime impact of convective transport and lightning NO_x production over North America: modeling dependence on meteorological simulations. *Atmos. Chem. Phys.* **2009**, *9*, 4315–4327.

(18) Wang, Y.; Choi, Y.; Zeng, T.; Ridley, B.; Blake, N.; Blake, D.; Flocke, F. Late-spring increase of trans-Pacific pollution transport in the upper troposphere. *Geophys. Res. Lett.* **2006**, *33*, L0181110.1029/2005GL024975.

(19) Zeng, T.; Wang, Y.; Chance, K.; Blake, N.; Blake, D.; Ridley, B. Halogen-driven low altitude O₃ and hydrocarbon losses in spring at northern high latitudes. *J. Geophys. Res.* **2006**, *111*, D1731310.1029/2005JD006706.

(20) Choi, Y.; Wang, Y.; Yang, Q.; Cunnold, D.; Zeng, T.; Shim, C.; Luo, M.; Eldering, A.; Bucsela, E.; Gleason, J. Spring to summer northward migration of high O₃ over the western North Atlantic. *Geophys. Res. Lett.* **2008**, *35*, L0481810.1029/2007GL032276.

(21) Zhao, C.; Wang, Y.; Yang, Q.; Fu, R.; Cunnold, D.; Choi, Y. Impact of East Asian summer monsoon on air quality over China: View from space. *J. Geophys. Res.* **2010**, *115*, D0930110.1029/2009JD012745.

(22) Carter, W. P. L. *Development of the SAPRC-07 Chemical Mechanism and Updated Ozone Reactivity Scales*; Final Report to the California Air Resources Board Contract No. 03-318; Center for Environmental Research and Technology College of Engineering, University of California: CA, 2009; www.eos.ubc.ca/~bainslie/Carter_2009-SAPRC-07.pdf.

(23) Liu, Z.; Wang, Y.; Gu, D.; Zhao, C.; Huey, L. G.; Stichel, R.; Liao, J.; Shao, M.; Zhu, T.; Zeng, L.; Liu, S.-C.; Chang, C.-C.; Amoroso, A.; Costabile, F. Evidence of reactive aromatics as a major source of peroxy acetyl nitrate over China. *Environ. Sci. Technol.* **2010**, *44*, 7017–7022.

(24) Wang, Y.; Jacob, D. J.; Logan, J. A. Global simulation of tropospheric O₃-NO_x-hydrocarbon chemistry. 3. Origin of tropospheric ozone and effects of non-methane hydrocarbons. *J. Geophys. Res.* **1998**, *103*, 10757–10768.

(25) Yienger, J. J.; Levy, H., II Empirical model of global soil-biogenic NO_x emissions. *J. Geophys. Res.* **1995**, *100*, 11,447–11,464.

(26) Zhang, Q.; Streets, D. G.; Carmichael, G. R.; He, K. B.; Huo, H.; Kannari, A.; Klimont, Z.; Park, I. S.; Reddy, S.; Fu, J. S.; Chen, D.; Duan, L.; Lei, Y.; Wang, L. T.; Yao, Z. L. Asian emission in 2006 for the NASA INTEX-B mission. *Atmos. Chem. Phys.* **2009**, *9*, 5131–5153.

(27) Gustafson, W. I., Jr.; Leung, L. R. Regional downscaling for air quality assessment: a reasonable proposition? *Bull. Am. Meteorol. Soc.* **2007**, *88*, 1215–1227.

(28) Song, J.; Lei, W.; Bei, N.; Zavala, M.; de Foy, B.; Volkamer, R.; Cardenas, B.; Zheng, J.; Zhang, R.; Molina, L. T. Ozone response to emission changes: a modeling study during the MCMA-2006/MILAGRO Campaign. *Atmos. Chem. Phys.* **2010**, *10*, 3827–3846.

(29) Kanaya, Y.; Fukuda, M.; Akimoto, H.; Takegawa, N.; Komazaki, Y.; Yokouchi, Y.; Koike, M.; Kondo, Y. Urban photochemistry in central Tokyo: 2. Rates and regimes of oxidant ($O_3 + NO_2$) production. *J. Geophys. Res.* **2008**, *113*, D0630110.1029/2007JD008671.

(30) Lin, J.-T.; Wuebbles, D. J.; Huang, H.-C.; Tao, Z.; Caughey, M.; Liang, X.-Z.; Zhu, J.-H.; Holloway, T. Potential effects of climate and emissions changes on surface ozone in the Chicago area. *J. Great Lakes Res.* **2010**, *36*, 59–6410-1016/j.jglr.2009.09.004.

(31) Streets, D. G.; Fu, J. S.; Jang, C. J.; Hao, J.; He, K.; Tang, X.; Zhang, Y.; Wang, Z.; Li, Z.; Zhang, Q.; Wang, L.; Wang, B.; Yu, C. Air quality during the 2008 Beijing Olympic Games. *Atmos. Environ.* **2007**, *41*, 480–492.